

Contributions of the 12 Neuron Classes in the Fly Lamina to Motion Vision

John C. Tuthill,^{1,2,3} Aljoscha Nern,^{1,2} Stephen L. Holtz,¹ Gerald M. Rubin,¹ and Michael B. Reiser^{1,*}

¹HHMI/Janelia Farm Research Campus, 19700 Helix Drive, Ashburn, VA 20147, USA

²These authors contributed equally to this work

³Present address: Department of Neurobiology, Harvard Medical School, 220 Longwood Avenue, Boston, Massachusetts 02115, USA

*Correspondence: reiser@m@janelia.hhmi.org

<http://dx.doi.org/10.1016/j.neuron.2013.05.024>

SUMMARY

Motion detection is a fundamental neural computation performed by many sensory systems. In the fly, local motion computation is thought to occur within the first two layers of the visual system, the lamina and medulla. We constructed specific genetic driver lines for each of the 12 neuron classes in the lamina. We then depolarized and hyperpolarized each neuron type and quantified fly behavioral responses to a diverse set of motion stimuli. We found that only a small number of lamina output neurons are essential for motion detection, while most neurons serve to sculpt and enhance these feedforward pathways. Two classes of feedback neurons (C2 and C3), and lamina output neurons (L2 and L4), are required for normal detection of directional motion stimuli. Our results reveal a prominent role for feedback and lateral interactions in motion processing and demonstrate that motion-dependent behaviors rely on contributions from nearly all lamina neuron classes.

INTRODUCTION

Fly motion detection is a key model system for studying fundamental principles of neural computation. Flies exhibit robust visual behaviors (Heisenberg and Wolf, 1984), and neurons in the fly visual system are highly sensitive to visual motion stimuli (Hausen, 1982). A mathematical model for visual motion detection, the Hassenstein-Reichardt elementary motion detector (HR-EMD; Hassenstein and Reichardt, 1956), successfully reconciles a wide range of behavioral and electrophysiological phenomena measured in flies (Egelhaaf and Borst, 1989; Götz, 1964; Haag et al., 2004; Hausen and Wehrhahn, 1989). The basic operation of the HR-EMD is a multiplication of two input signals after one of them has been temporally delayed (Figure 1B; Reichardt, 1961). The “correlation-type” structure of the HR-EMD is highly similar to models for motion detection in the vertebrate retina (Borst and Euler, 2011) and may represent a common neural computation across sensory systems (Carver et al., 2008).

In spite of the success of the EMD model, its cellular implementation remains unknown. There is evidence that EMD motion

computation is implemented locally, between neighboring retinotopic subunits of the fly eye (Buchner, 1976, 1984) and that local motion signals are then spatially integrated within motion-sensitive tangential neurons in downstream circuits (Figure 1B; Krapp et al., 1998; Single and Borst, 1998; Single et al., 1997). However, it is unclear if the computational nodes of the HR-EMD, the delay filter and the multiplier, correspond to individual cell types, or if motion detection is computed in a more distributed manner, with distinct contributions from many different neurons. It is also possible that there are multiple circuits dedicated to motion computation; different neuron types could extract specific visual features, as in vertebrate retinal ganglion cells (Gollisch and Meister, 2010), and compute motion independently within parallel channels. Indeed, several recent studies suggest that fly motion vision may be segregated into parallel, functionally distinct channels (Clark et al., 2011; Eichner et al., 2011; Joesch et al., 2010; Katsov and Clandinin, 2008; Rister et al., 2007).

The fly visual system consists of four ganglia called the lamina, medulla, lobula, and lobula plate (Figure 1A), which together are referred to as the optic lobes. As the first synaptic relay between the photoreceptors and motion-sensitive tangential neurons in the lobula plate, it has been hypothesized that the early stages of motion computation may occur in the lamina (Coombe et al., 1989; Douglass and Strausfeld, 1995). The lamina is organized into an array of ~750 retinotopic “cartridges,” each of which corresponds to a discrete sample of the visual world, ~5° in *Drosophila* (Braitenberg, 1967; Buchner, 1971; Kirschfeld, 1967). The anatomy and connectivity of lamina neurons is known in exquisite detail, owing to detailed Golgi studies (Fischbach and Dittrich, 1989) and electron microscopy (EM) reconstructions (Meinertzhagen and O’Neil, 1991; Rivera-Alba et al., 2011). Six light-sensitive photoreceptors, R1–R6, project their axons into each lamina cartridge. Two other photoreceptor neurons, R7 and R8, pass through the lamina and synapse in specific layers of the medulla.

Besides the photoreceptor axons, the lamina also contains processes of 12 other neuronal cell types (Figures 1C and 1D). These lamina-associated neurons include five lamina output neurons, six putative feedback neurons, and one lamina intrinsic cell (Fischbach and Dittrich, 1989). Eight of these neuron classes are columnar—there is one cell per retinotopic column (Figure 1C). The columnar neurons include the feedforward lamina monopolar cells, L1–L5 (Figure 1C, red), which send axonal processes into the medulla. The largest of the monopolar cells, L1,

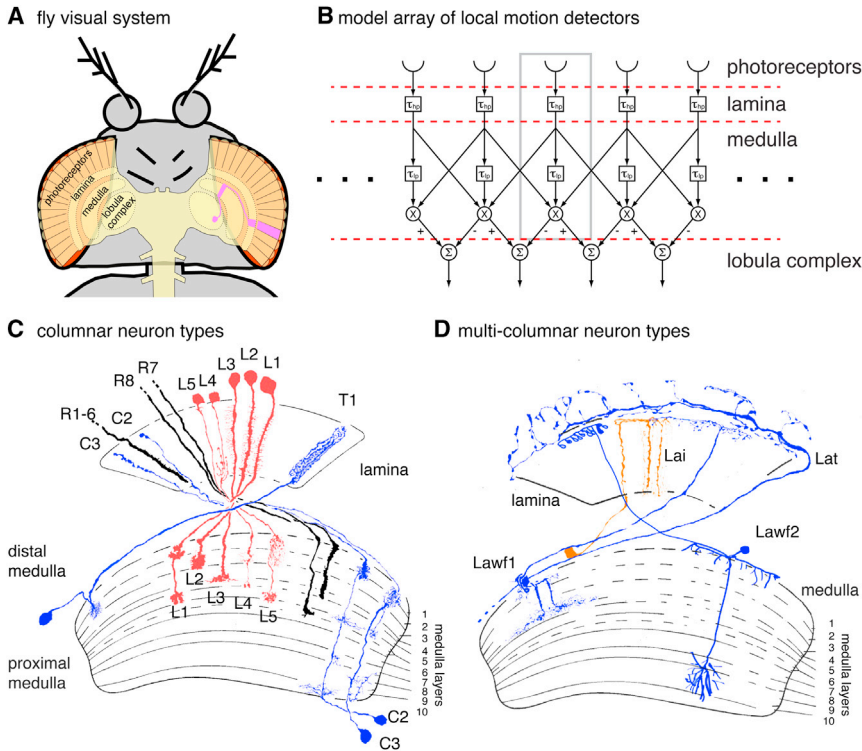


Figure 1. Overview of the Fly Visual System and Its Proposed Role in Local Motion Computation

(A) In the early visual system of *Drosophila*, input from photoreceptor neurons in the retina is initially processed in the optic lobes, which consist of a series of optic ganglia called the lamina, medulla, and lobula complex (comprising the lobula and lobula plate). Optic lobe neuropils are organized as arrays of retinotopic columns. One series of columns is highlighted in pink.

(B) A schematic of an array of HR-EMDs, the classical computational model for local motion detection in the optic lobes. In this typical implementation, visual input passes from photoreceptors and is temporally filtered in the lamina. Motion detection is then performed by mirror-symmetric subunits, each multiplying the incoming signal with a time-delayed version from neighboring columns. This computation is commonly believed to occur within the medulla. The gray rectangle outlines a single columnar unit within the model, which corresponds to a single anatomical column within the lamina and medulla.

(C) The columnar neurons with synaptic connections in the lamina. Lamina output neurons L1–L5 are shown in red and putative feedback neurons from the medulla (C2, C3, T1) in blue. Photoreceptor neurons are also illustrated (gray). These neurons are present in all lamina columns, and single example profiles are shown arrayed across the lamina and medulla. This figure is adapted from Golgi drawings by Fischbach and Dittrich (1989).

(D) The multicolumnar neurons with processes in the lamina. These neurons are present with less than one cell per column, but as a population their arbors cover the entire visual field. Lamina intrinsic neurons (Lai; orange) are confined to the lamina. Lamina wide-field neurons (Lawf1, Lawf2; blue) provide feedback from the medulla to the distal lamina. Lamina tangential neurons (Lat; blue) arborize even more distal in the region of lamina neuron cell bodies. Lat cell bodies (data not shown) are located between the optic lobe and central brain near the accessory medulla. Lat cells also arborize in the ipsilateral central brain and the accessory medulla (data not shown). Like (C), this figure is adapted from Fischbach and Dittrich (1989), except for Lawf2, which was drawn based on single-cell labeling data obtained in this study (see Figure 2J).

L2, and L3, receive direct synaptic input from the R1–R6 photoreceptors, but L4 and L5 do not (Meinertzhagen and O’Neil, 1991; Rivera-Alba et al., 2011). In addition to these five lamina output neurons, three putative feedback neurons, T1, C2, and C3, are also columnar (Figure 1C, blue). These neurons have cell bodies in the medulla and send their axons back to the lamina. EM studies have shown that C2 and C3 are presynaptic on several cell types in the lamina (Meinertzhagen and O’Neil, 1991; Rivera-Alba et al., 2011). By contrast, no synaptic targets are currently known for T1 neurons.

Four other lamina-associated neuron classes are multicolumnar: there is less than one neuron per lamina column, and the arbors of each neuron span multiple columns (Figure 1D). With the exception of the lamina intrinsic amacrine neurons (Lai), which are confined to the lamina, the anatomy of these multicolumnar neurons suggests that they function as feedback neurons. Wide-field feedback from the medulla to the lamina is provided by two types of lamina wide-field neurons (Lawf1 and Lawf2). Lawf2, which was identified in the course of the present study and was also recently reported elsewhere (Hasegawa et al., 2011), can be clearly distinguished from Lawf1 by its layer specificity in the medulla (Figure 1D). Finally, lamina tangential neurons (Lat), approximately four cells per optic lobe, project

from the ipsilateral central brain to the distal surface of the lamina. These neurons do not innervate the medulla proper but have arborizations in the accessory medulla, a small medulla-associated neuropil thought to function in the control of circadian rhythms (Helfrich-Förster et al., 2007).

Several studies have investigated the functional roles of the large monopolar cells, L1 and L2. L1 and L2 are together required for motion detection. Simultaneously silencing both neuron types eliminates behavioral (Clark et al., 2011; Rister et al., 2007) and electrophysiological (Joesch et al., 2010) responses to motion, while silencing each cell type individually has been reported to cause differential responses to progressive and regressive motion at low contrasts (Rister et al., 2007), contrast-inverting edges (Clark et al., 2011), and motion stimuli defined by brightness increments and decrements (Joesch et al., 2010). Electrophysiological recordings (Laughlin and Hardie, 1978; Zheng et al., 2006) and calcium imaging studies (Clark et al., 2011) have found that the physiological responses of L1 and L2 are largely similar. Both are nonspiking neurons that respond to luminance increases with a transient hyperpolarization and luminance decreases with a transient depolarization. Neither L1 nor L2 is selective for moving stimuli. Overall, these data suggest that L1 and L2 provide input to

motion circuits but are not directly involved in elementary motion computation.

In comparison to L1 and L2, little is known about the contributions of the other ten lamina-associated neuron types. This is primarily because the small size of these neurons has, except for a few examples in larger flies (Douglass and Strausfeld, 1995), prevented electrophysiological recording. Specific GAL4 driver lines for these remaining neuron types have also not been available for behavioral genetics studies. In this Article, we use intersectional genetic strategies to build a collection of driver lines that target each of the 12 lamina-associated neuron types. We then genetically silence and activate each lamina neuron type and evaluate the consequences on behavioral responses to a panel of visual stimuli. Our results provide evidence that most lamina-associated neurons contribute to motion processing and that the HR-EMD model describes the emergent properties of a complex circuit, rather than discrete arithmetic operations implemented by a small number of individual neuron types.

RESULTS

Construction of Specific GAL4 Driver Lines for Individual Lamina Neuron Types

We first surveyed a large collection of imaged GAL4 lines (Jenett et al., 2012; Pfeiffer et al., 2008) for expression in the *Drosophila* lamina and further examined expression patterns of selected lines by reimagining at higher resolution or with single-cell labeling techniques. Individual lamina neuron types could be identified in this screen by their distinct stereotyped morphology using both the overall expression pattern and single-cell labeling (Figure 2). Our screen revealed multiple drivers for each of the lamina-associated neuron types. However, similar to available GAL4 lines, such as lines widely used in the study of L1 and L2 function (Figure S1 available online; Clark et al., 2011; Gao et al., 2008; Joesch et al., 2010; Katsov and Clandinin, 2008; Rister et al., 2007), most of these driver lines had expression in other cell types of the optic lobes, central brain, or ventral nerve cord. We therefore used the intersectional Split-GAL4 method (Luan et al., 2006; Pfeiffer et al., 2010) to further refine expression patterns. In this method, two parts of the GAL4 transcription factor, the activation domain (AD) and DNA-binding domain (DBD), are expressed in the two patterns to be intersected. Functional GAL4 is only reconstituted in cells that express both the AD and DBD, ideally resulting in a specific driver targeting only the cell population of interest.

Taking advantage of the modular nature of the enhancer-GAL4 collection (Jenett et al., 2012; Pfeiffer et al., 2008), we generated multiple AD and DBD drivers with predicted expression in each lamina cell type. We then assayed the expression patterns of more than 100 AD/DBD combinations and selected suitable lines for further use. For 10 of the 12 types of lamina neurons, we identified at least two Split-GAL4 driver lines with high specificity (Table S1). Figure 2 shows the expression patterns for one line of each cell type, as well as example images of single labeled cells that summarize the critical identifying anatomical features (images of the additional Split-GAL4 lines and ventral nerve cord expression of all lines are available on the authors' website: <http://www.janelia.org/lab/reiser-lab>). We confirmed the cell-type expression of these lines by imaging UAS-EGFP-Kir2.1

expression patterns (Figure S3A). For L1, the identified lines showed variable levels of incomplete expression (Figures 2A' and 2A'') and only one such line was examined (we note that the UAS-EGFP-Kir2.1 expression pattern appeared more complete, Figure S3A). We detail the completeness of expression within each line in Table S1. We also tested one lamina tangential (Lat) line and lines that drove expression in two important cell-type combinations (L1/L2 and C2/C3). The advantage of using two highly specific drivers in functional studies is that the common phenotypic effects of driving neural effectors with different Split-GAL4 combinations can be confidently attributed to perturbation of the lamina-associated neurons.

Manipulating Lamina Neurons Affects Visual Behavior

During flight, flies rely on vision to maintain course control, avoid collisions, and orient toward objects (Heisenberg and Wolf, 1984). Quantifying flight steering is a sensitive way to measure visually evoked behaviors (Götz, 1964; Heisenberg and Wolf, 1984). For this reason, we examined visual behavior in tethered flying flies positioned within a cylindrical LED arena (Figure 3A; Reiser and Dickinson, 2008). In the flight arena, we used an optical wing-beat analyzer (Götz, 1987) to measure yaw steering responses to an extensive set of open- and closed-loop visual stimuli (Figures 3A, 3B, and S2). We tested several classic visual stimuli, such as large-field (optomotor) gratings of varying spatial frequency, velocity, and contrast (Duistermars et al., 2007a; Götz, 1964), small-field stripe patterns that oscillated at high and low frequencies (Duistermars et al., 2007b; Reichardt and Wenking, 1969), and motion stimuli that mimicked the optic flow patterns encountered by flies during flight (Theobald et al., 2010). We also designed novel stimuli to test specific hypotheses about lamina function, such as selectivity for progressive (front-to-back) versus regressive (back-to-front) motion (Duistermars et al., 2012; Rister et al., 2007), rotation versus expansion (Duistermars et al., 2007a; Katsov and Clandinin, 2008), and ON versus OFF motion signals (Clark et al., 2011; Joesch et al., 2010). Finally, we adapted several psychophysical techniques used to study early vision in other systems, such as reverse-phi motion (Anstis and Rogers, 1975; Tuthill et al., 2011) and contrast nulling (Cavanagh and Anstis, 1991; Chichilnisky et al., 1993; Smear et al., 2007). All of these stimuli were interleaved within a single protocol that required ~40 min of sustained flight behavior. A complete description of the visual stimuli used in this study is included in Figure S2 and described in the Supplemental Experimental Procedures.

In order to test the functional role of each lamina-associated neuron type in peripheral visual processing, we genetically expressed an inwardly rectifying K⁺ channel, Kir2.1, which suppresses synaptic activity by hyperpolarizing the resting potential (Baines et al., 2001). Consistent with previous findings (Clark et al., 2011; Joesch et al., 2010; Rister et al., 2007), expression of Kir2.1 in both L1 and L2 abolished fly turning responses to visual motion stimuli, such as the rotation of a wide-field grating and the oscillation of a dark stripe (Figures 3B and 3C). Because the Kir2.1 channel was tagged with GFP, we were able to confirm the expression in the Split-GAL4 lines by confocal microscopy (Figures S3A and S3B). We also verified that Kir2.1 expression effectively silenced light-evoked electrical activity

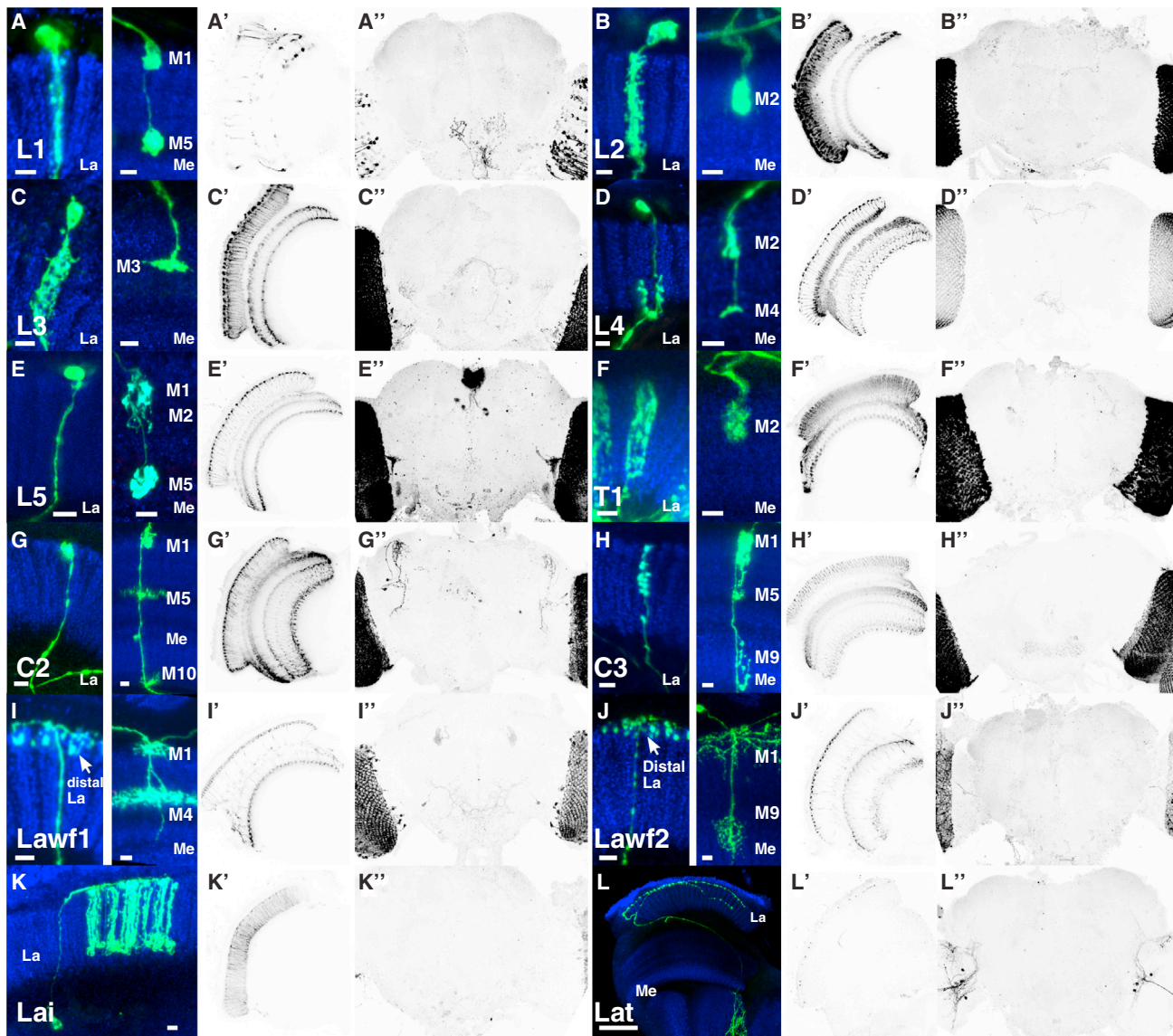


Figure 2. Each of the 12 Neuron Classes in the Fly Lamina Was Targeted Using the Split-GAL4 Technique

Shown for each cell type are the following: single cell images illustrating defining features of each neuron class (A–L), a confocal section through an optic lobe of one Split-GAL4 driver (A'–L'), and a maximum intensity projection of expression in the central brain of the same Split-GAL4 line (A''–L''). Expression patterns were visualized by confocal microscopy using UAS-driven expression of a membrane-targeted GFP and anti-GFP antibody staining (detailed in [Supplemental Experimental Procedures](#)). Blue labeling in single cell images shows a presynaptic marker (Brp; Nc82 antibody staining). Layer positions of terminals in the medulla are indicated as M1, M2, etc. in (A)–(L). For example, L1 has medulla terminals in layers M1 and M5 and L2 in layer M2. Each of the lamina-associated neurons can be unambiguously identified by these anatomical features. Specific drivers used for each image are listed in [Table S1](#). Ventral nerve cord expression patterns and images of the remaining Split-GAL4 lines are available on the authors' website. Scale bars represent 50 μm in (A'), (A''), and (L), and 5 μm in all others.

through targeted whole-cell patch-clamp recordings from Lawf2 neurons (Figure S3C). In a complementary set of experiments, we genetically expressed the temperature-gated cation channel dTrpA1 (Hamada et al., 2008), which depolarizes *Drosophila* neurons (Pulver et al., 2009).

We compared the behavioral responses of experimental Split-GAL4 lines crossed to UAS-Kir2.1 to the responses of four control lines (each an individual Split-GAL4 half crossed to UAS-Kir2.1). The behavioral responses of these control lines

were indistinguishable and were pooled. For most cell types, we tested more than one Split-GAL4 line and then employed a statistical analysis to control for false discovery rate (Benjamini and Hochberg, 1995). For each cell type and for each stimulus condition, we report as significant only those cases in which both of the Split-GAL4 lines that target each cell type pass our statistical criterion (see [Supplemental Experimental Procedures](#) for details). Although statistical tests were always performed on individual Split-GAL4 lines, we display behavioral response data

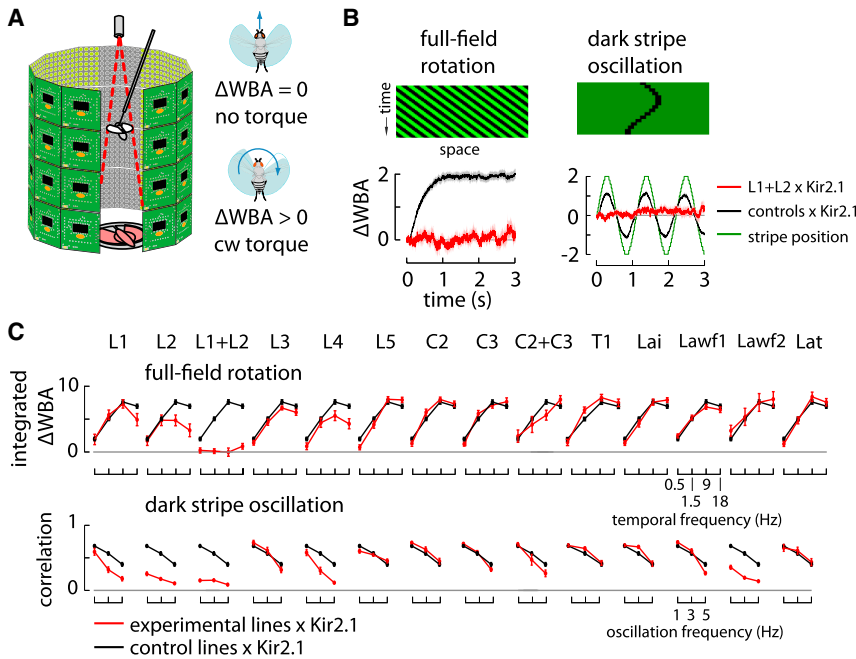


Figure 3. Silencing or Activating Specific Lamina Neurons Alters Fly Visual Behavior in a Virtual Reality Flight Simulator

(A) A flying fly is suspended within an LED arena in which the amplitude of each wing beat is tracked by an optical detector. The difference between the two wing-beat amplitudes (Δ WBA) is proportional to yaw torque. For example, when the amplitude of the left wing beat is greater than the right, the fly is attempting to steer to the right with clockwise torque.

(B) Example flight steering responses (mean \pm SEM) to rotation of a full-field stimulus ($90^\circ/\text{s}$ corresponding to a temporal frequency of 3 Hz, left) and oscillation of a dark stripe (started at the center of the arena and oscillated between $\pm 37.5^\circ$ at 0.9 Hz, right). Silencing both L1 and L2 neurons with Kir2.1 abolishes behavioral responses to full-field and small-field motion stimuli. The space-time diagrams illustrate the luminance patterns displayed to the fly in the arena.

(C) Behavioral tuning curves for two motion stimuli across all experimental genotypes. The results for each experimental line (or average of two lines), crossed to Kir2.1, are shown in red, while the results for the control flies are shown in black (see text for details). Top: mean

integrated steering responses (\pm SEM) to a full-field rotation stimulus (30° spatial period) at four temporal frequencies. Bottom: fly responses to oscillation of a dark stripe at three frequencies. Tuning curves show the mean correlation (\pm SEM) between the stimulus position and the Δ WBA.

in Figures 3, 4, 5, 6, and 7 as the average of all lines tested for each cell type.

We found that silencing most lamina neurons had subtle effects on basic visual behaviors, such as the wide-field optomotor responses and small-field stripe tracking (Figure 3C). However, testing fly responses to many unique visual stimuli revealed that some cell types contribute to motion detection under specific stimulus conditions. The difference between wild-type responses to all of the stimuli we tested and the responses of flies in which we have manipulated each lamina cell type are summarized with color-coded levels of statistical significance in Figure 4A. In this results matrix, each row represents the targeted neuron class, while each column is a separate visual stimulus condition (visual stimuli are detailed in Figure S2 and Supplemental Experimental Procedures). The color and intensity of each cell indicates whether Kir2.1 expression significantly affected fly behavior. The behavioral results summarized in Figure 4 are elaborated for a few cell types in Figures S5 and S7; the complete data set is available on the authors' website (<http://www.janelia.org/lab/reiser-lab>).

The strongest phenotypes we observed were for the primary lamina output neurons, L1 and L2 (top three rows of Figure 4A). Silencing either of these cell types significantly affected fly responses to many different behavioral conditions, supporting the hypothesis that these neurons are the primary feedforward inputs to downstream motion circuits. A previous report has suggested that L1 and L2 support detection of motion generated by luminance increments and decrements, respectively (Joesch et al., 2010). We found that silencing L2 neurons significantly altered fly responses to a decreasing luminance gradient but did not affect tracking of moving dark edges (ON and OFF

motion stimuli in Figures 4A and S5B). Silencing L1 neurons did not affect fly response to either of these stimuli (Figures 4A and S5A), but more subtle deficits for L1 inactivation were seen in further experiments (Figure S6).

Apart from L1 and L2, the phenotypic effects were much sparser for secondary lamina output neurons and lamina-associated feedback neurons. Silencing most neuron types specifically affected fly responses to a small number of visual behaviors (bottom nine rows of Figure 4A), indicating specialized roles for these neurons. These behavioral phenotypes were largely consistent across different Split-GAL4 combinations (Figure S4), strongly suggesting that behavioral effects were due to Kir2.1 expression in lamina neurons rather than off-target consequences of our genetic manipulations. This is corroborated by the fact that silencing some neuron classes, such as L5, had no measurable effect on the behaviors we tested. Likewise, some visual behaviors, such as orientation toward a lateral flickering stripe, were entirely unaffected by silencing any of the 12 neuronal types. It is possible that such behaviors are mediated in part by input from the R7 and R8 photoreceptors that bypass the lamina and terminate in the medulla.

We also tested a subset of behaviors while depolarizing neurons by heat activation of dTrpA1. Surprisingly, dTrpA1 expression in the primary lamina output neurons, L1 and L2, did not dramatically impair visual motion detection (Figure 4B). However, in several instances, when expressed in other neurons, dTrpA1 expression altered fly behavior in unexpected ways. For example, depolarizing T1 neurons dramatically reduced the flight steering responses to most visual stimuli tested (Figure 4B). T1 cells are a mysterious type of columnar neurons that, based on EM reconstructions, appear to be exclusively postsynaptic

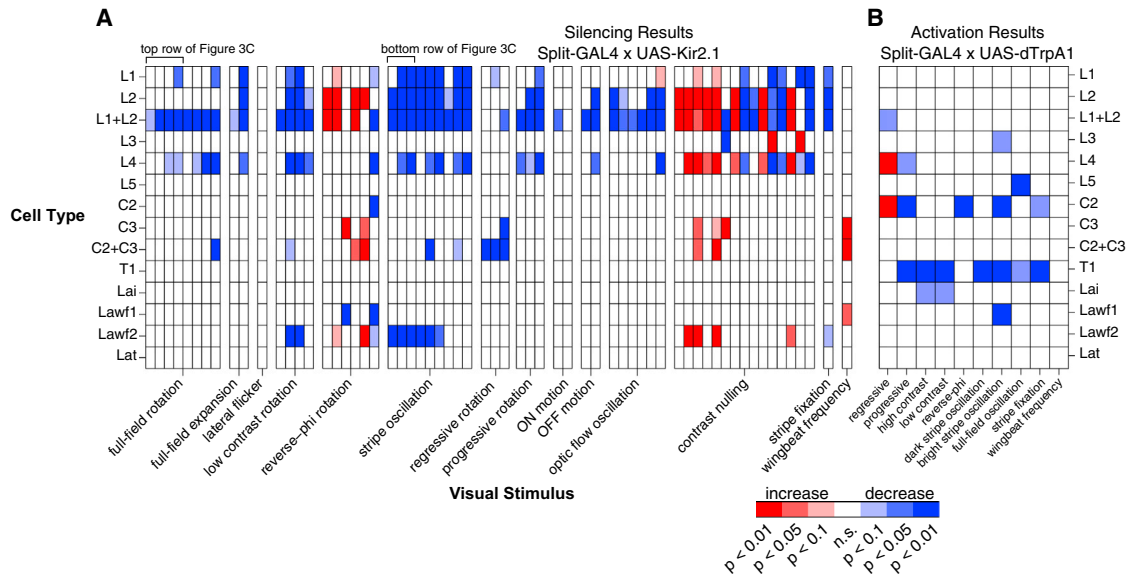


Figure 4. Summary of Behavioral Results for All Lamina Neurons

(A) The results of silencing each class of neurons are summarized as a heatmap, where each node represents the summary p value for the comparison between the experimental and control genotypes. The visual stimuli corresponding to each column are shown in Figure S2. Red (and blue) indicates a numerical increase (and decrease) in the test metric as determined by the signed difference between the mean of the test metric for each cell type and the mean of the control set. The p values corresponding to each line are shown in Figure S4 and have been aggregated for each cell type here. See Supplemental Experimental Procedures for details of the statistical procedure.

(B) Heatmap summary of all stimuli and lines tested using dTrpA1. Each cell represents the summary p value for comparisons between experimental and control genotypes (GAL4AD; GAL4DBD/UAS-dTrpA1 at 21°C and GAL4AD; UAS-dTrpA1 at 28°C). Specific Split-GAL4 lines tested are listed in Table S1.

in both the lamina (Meinertzhagen and O'Neil, 1991; Rivera-Alba et al., 2011) and the medulla (Takemura et al., 2008). Our data suggest that T1 neurons interact extensively with other lamina cell types, perhaps through gap junctions not resolvable by electron microscopy and that tonic depolarization of these cells is sufficient to disrupt basic visual behaviors.

Overall, we observed at least one phenotype for each lamina neuron type except for the lamina tangential cell (Lat). In several cases (L5, T1, Lai), neuronal silencing had no measurable effect on the behaviors we tested (Figure 4A), while activation using dTrpA1 significantly affected behavior (Figure 4B). For the remainder of the paper, we will focus on behavioral phenotypes related to specific aspects of spatial and temporal processing.

Role of Lamina Neurons in Directionally Selective Steering

The optic flow a fly experiences as it flies forward is predominantly progressive, moving from front-to-back across both eyes (Figure 5A). When presented with either progressive or regressive motion restricted to a single eye, tethered flying flies respond by turning in the direction of stimulus motion (Götz, 1968), although responses to regressive motion are weaker (Duistermars et al., 2012; Heisenberg, 1972; Tammero et al., 2004). In comparison, freely walking flies respond more robustly to regressively moving objects (Zabala et al., 2012). Despite behavioral evidence that the visual system differentiates regressive from progressive motion, the neuronal origin of these asymmetries is unknown. Such asymmetries could arise from

nonuniform spatial integration of local motion signals in the lobula plate (Krapp et al., 1998; Single and Borst, 1998; Single et al., 1997) or from nonlinear binocular interactions of lobula plate tangential neurons (Farrow et al., 2006; Krapp et al., 2001). It has also been proposed that directional asymmetries originate earlier in the visual system, perhaps in the lamina (Katsov and Clandinin, 2008; Rister et al., 2007). Our experiments identified four columnar lamina neurons that contribute to processing asymmetric motion signals moving either progressively or regressively across the eye (Figures 5A and 5B).

L4 neurons are unique among the lamina output neurons in that they interact with neighboring retinotopic columns within the lamina (Figure 5B). Within each lamina cartridge, L4 receives synaptic input from L2. In addition, each L4 neuron sends collaterals into posterior lamina cartridges (Strausfeld and Campos-Ortega, 1973), which synapse on both L2 and L4 neurons (Meinertzhagen and O'Neil, 1991; Rivera-Alba et al., 2011). In the medulla, L4 axons provide input to retinotopically posterior columns (Takemura et al., 2011). Based on this anatomical organization, it was proposed that the L2/L4 circuit mediates the detection of progressive motion (Braitenberg and Debbage, 1974; Takemura et al., 2011; Zhu et al., 2009).

Consistent with this prediction, we found that silencing L4 neurons impaired fly responses to monocular progressive but not regressive motion (Figure 5I). Silencing L2 neurons, the primary presynaptic input to L4, also altered fly responses to progressive but not regressive motion (Figure 5J), consistent with a previous report (Rister et al., 2007). Surprisingly, acute depolarization of

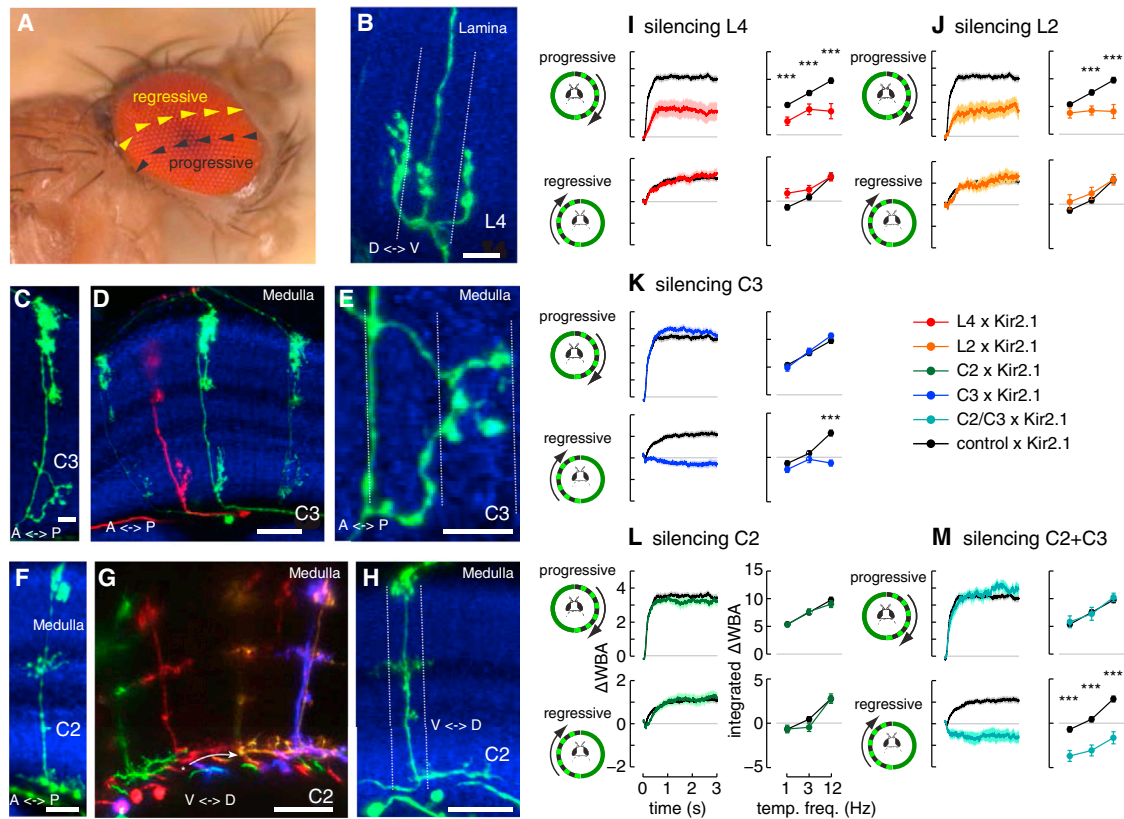


Figure 5. Silencing Four of the 12 Lamina-Associated Neuron Types Results in Directionally Asymmetric Changes to Fly Visual Perception

(A) Flies respond differently to visual motion presented in either the regressive (back-to-front) or progressive (front-to-back) directions.
 (B) L4 branches in the proximal lamina possess a characteristic, column-crossing arborizations. Dotted lines indicate approximate positions of column boundaries based on anti-Brp (Nc82) antibody staining (blue).
 (C–E) C3 neurons have multicolumnar directional branches in the proximal medulla.
 (C) Medulla arborizations of a single C3 neuron.
 (D) Stereotyped orientation of C3 branches. Multiple examples of C3 neurons in the same medulla visualized by multicolor stochastic labeling (details in Supplemental Experimental Procedures). Note that arbors in the proximal medulla consistently point in the posterior direction.
 (E) C3 arbors in M9 are multicolumnar as shown by a higher-magnification view of branches of the individual C3 neuron in (C).
 (F–H) C2 neurons are also multicolumnar and often have directional processes (for more examples, see Figure S3D).
 (F) A single cell flip-out of a C2 neuron shows C2 arborizations in different medulla layers.
 (G) Multicolor stochastic labeling of multiple C2 neurons in the same optic lobe showing similar oriented processes (along the DV axis) in M10. White arrow indicates approximate direction and length of one of these oriented processes.
 (H) A single C2 cell viewed along the DV axis shows a pronounced asymmetry in layer M10. Dotted lines indicate approximate positions of column boundaries. Scale bars represent 5 μm in (B), (C), and (E), 10 μm in (F), and 20 μm (D), (G), and (H).
 (I–M) Fly responses to monocularly restricted progressive motion are significantly reduced by Kir2.1 expression in L4 (I) and L2 (J), but not C2 (K) or C3 (L). Conversely, silencing C3 (L) or both C2 and C3 (M) reduced fly responses to regressive motion. All steering responses (mean \pm SEM) to a lateral optomotor stimulus ($\lambda = 30^\circ$) rotating progressively at $360^\circ/\text{s}$ (12 Hz). Right: mean integrated turn responses to progressive motion at three speeds ($n \geq 10$ flies per genotype; *** $p < 0.01$, ** $p < 0.05$; t tests on maximum p values, corrected for multiple comparisons; see Supplemental Experimental Procedures for details).

L4 neurons by dTrpA1 expression decreased fly responses to progressive motion and increased responses to regressive motion stimuli (Figures 4B and S7A). These results demonstrate that silencing L4 neurons alters detection of progressive motion across the eye and that silencing its primary lamina input, L2, has a similar effect.

In addition to affecting progressive motion responses, silencing L2 and L4 produced several other behavioral phenotypes. Kir2.1 expression in L2 neurons dramatically affected most motion behaviors tested (Figures 4A and S5B), consistent with its role as one of the primary feedforward inputs to down-

stream motion circuits (Clark et al., 2011; Joesch et al., 2010; Rister et al., 2007). Silencing L4 neurons also decreased full-field optomotor responses at low contrasts and very fast stimulus speeds and impaired the ability of flies to track rapidly oscillating patterns (Figure S7A).

In contrast to L2 and L4, we found that the columnar, centrifugal neurons C2 and C3 play an important role in shaping behavioral responses to regressive motion stimuli. C2 and C3 are GABAergic neurons (Fei et al., 2010; Kolodziejczyk et al., 2008) that arborize in multiple layers of the proximal and distal medulla and send axons into the lamina, where they are primarily

presynaptic on several neuron types, including L1, L2, and Lai neurons (Meinertzhagen and O'Neil, 1991; Rivera-Alba et al., 2011). In the distal medulla, C2 and C3 both receive presynaptic input from L1 and form synapses on L2; C2 is also presynaptic to L1 (Takemura et al., 2008).

In addition to the distal medulla, C3 neurons arborize in the proximal medulla, primarily in layer M9 (Figures 1C and 2H). Examination of the C3 terminals in the medulla revealed that putative dendritic arbors in layer M9 showed a stereotyped orientation, with processes extending posteriorly from the branch point off the main axon (Figures 5C and 5D). This directionality was highly stereotyped (33/33 neurons from 3 brains). Closer examination revealed that these arbors extend into neighboring columns (Figure 5E), reminiscent of the multicolumnar projections of L4 in lamina (Figure 5B; Strausfeld and Campos-Ortega, 1973) and medulla (Takemura et al., 2011). This organization suggests that C3 neurons receive synaptic input from posterior medulla columns and provide output to more anterior lamina and medulla columns. Such an asymmetric circuit could enhance the detection of regressive motion by amplifying signals translating from posterior to anterior across the eye. Consistent with this hypothesis, we found that silencing C3 neurons abolished steering responses to regressive motion stimuli moving at high speeds (Figure 5K, bottom row) but did not affect responses to progressive motion (Figure 5K, top row) or basic optomotor stimuli (Figure S7C).

C2 neurons also had multicolumnar, presumably dendritic, arborizations in the medulla (Figures 5F–5H). Most of the C2 arbors in layer M10, while variable in their detailed shapes, were strongly asymmetric (18/20 neurons from 19 brains), extending preferentially in a dorsal direction relative to the main neurite (Figures 5G, 5H, and S3D). This multicolumnar profile of C2 neurons suggests that they may also be involved in integrating signals from neighboring columns. Silencing C2 neurons resulted in decreased fly responses to slow regressive motion (3 Hz) in only one of the two Split-GAL4 lines we tested (Figures 5L and S7B). However, depolarizing C2 neurons with dTrpA1 increased steering responses to regressive motion and decreased responses to progressive motion (Figures 4B and S7B).

In addition to examining the effect of silencing C2 and C3 neurons individually, we tested a Split-GAL4 line that targeted both centrifugal neurons. Remarkably, silencing both C2 and C3 neurons together dramatically shifted fly responses to all regressive motion stimuli, such that clockwise regressive motion caused flies to turn counterclockwise (Figure 5M, bottom row). However, behavioral responses to progressive motion were unaffected (Figure 5M, top row).

During forward flight, rapid feedback from the centrifugal neurons could actively enhance the coding of luminance signals moving regressively across the eye. Although the LMCs are not themselves sensitive to motion (Clark et al., 2011; Laughlin and Hardie, 1978; Reiff et al., 2010), C2 and C3 may contribute to asymmetric filtering of luminance signals via synapses within the lamina (Meinertzhagen and O'Neil, 1991; Rivera-Alba et al., 2011), through presynaptic inhibition at the LMC terminals in the proximal medulla (Takemura et al. 2008, 2011) or by providing input to unidentified downstream neurons in the medulla. The parallels between the phenotypes of C2 and C3

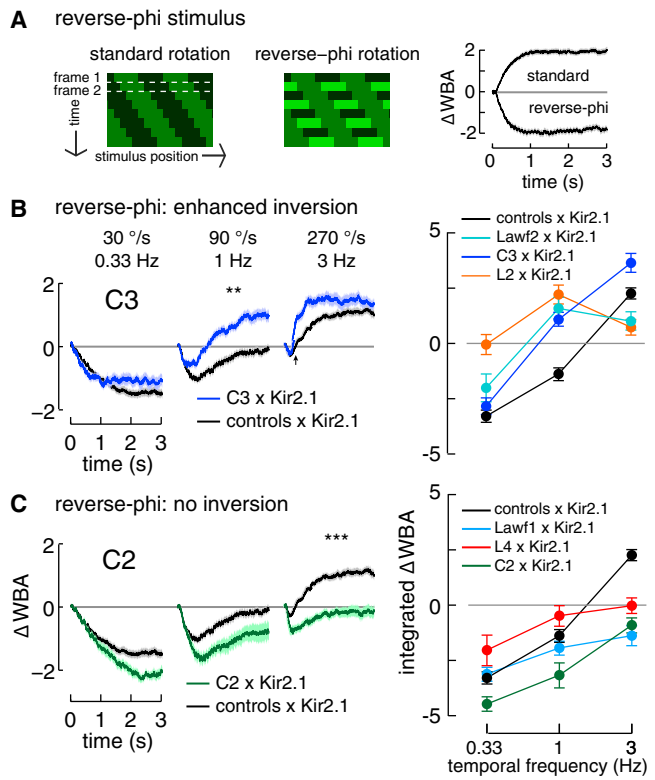


Figure 6. Lamina Neurons Differentially Contribute to Temporal Visual Processing

(A) Left: space-time depictions of reverse-phi and standard motion stimuli. Right: example steering responses to clockwise rotation of standard and reverse-phi motion stimuli ($\lambda = 30^\circ$, 12 Hz).

(B) Left: silencing C3 neurons increases the rate of the reverse-phi inversion. Time series are flight steering responses (mean \pm SEM) to rotation of a reverse-phi motion stimulus (90° spatial period) at three speeds. Right: mean integrated turn amplitude (\pm SEM) for cases in which silencing a class of lamina neurons increased reverse-phi inversion. The arrowhead marks the start of the reverse-phi inversion (see primary text).

(C) Same as in (B), except for cell types that eliminate the reverse-phi inversion.

suggest that they perform overlapping functional roles, perhaps each with distinct temporal and spatial properties.

Role of Lamina Neurons in Temporal Processing

To investigate how lamina neurons shape the temporal properties of fly vision, we compared tuning curves to standard and reverse-phi motion stimuli. Reverse-phi is a visual illusion that combines a contrast reversal with motion (Anstis and Rogers, 1975). Many species, including humans (Anstis and Rogers, 1975), perceive an illusory reversal in the direction of a reverse-phi motion stimulus. Flies typically turn in the direction opposite that of a reverse-phi motion pattern (Figure 6A)—they exhibit a “reverse-optomotor response” (Tuthill et al., 2011). However, very fast reverse-phi motion stimuli trigger transient reverse-optomotor steering, followed by compensatory turning in the opposite direction (Figure 6B, arrowhead). The timing and amplitude of these responses depend on the flicker rate of the reverse-phi stimulus and were predicted to arise from adaptation in peripheral circuits (Tuthill et al., 2011).

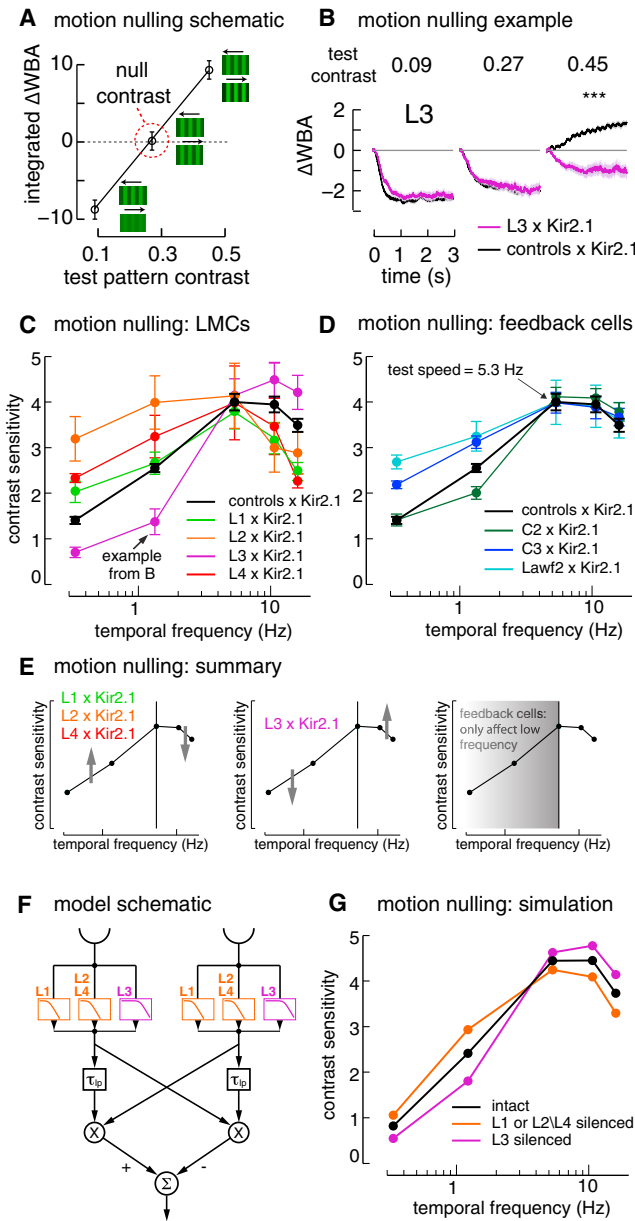


Figure 7. Motion Nulling Reveals Contributions of Lamina Neurons to Contrast Sensitivity as a Function of Stimulus Speed

(A) Nulling stimuli consist of two superimposed square-wave gratings (45° spatial period): a constant reference stimulus and a test stimulus whose contrast is varied across trials. At low test contrast, flies follow the reference stimulus ($\Delta WBA < 0$); at high test contrast, flies follow the test stimulus ($\Delta WBA > 0$). The null contrast is the contrast of the test stimulus needed to cancel, or “null,” the reference stimulus.

(B) Example of a motion nulling phenotype: silencing L3 neurons alters fly contrast sensitivity at low speeds. The reference stimulus has a relative contrast of 0.27 and rotates counterclockwise at 4 Hz, while the test stimulus rotates clockwise at 1.33 Hz and the contrast is varied across trials. Control flies follow the high-contrast test stimulus on the last trial, while flies with L3 silenced follow the reference stimulus.

(C) Tuning curves of contrast sensitivity (1/null contrast) measured over a range of test stimulus temporal frequencies. Silencing four of the lamina monopolar cells, L1–L4, alters contrast sensitivity tuning at both high and low frequencies.

We found that silencing several lamina cell types specifically altered the amplitude and timing of behavioral responses to reverse-phi motion (Figures 6B and 6C). One phenotypic class, which included the cell types C3, L2, and Lawf2, exhibited an enhancement of the reverse-optomotor inversion at high speeds. For example, silencing C3 neurons dramatically increased the speed and magnitude of the reverse-phi inversion (Figure 6B). Silencing the other type of centrifugal neurons, C2, had the opposite effect, increasing the magnitude of reverse-optomotor responses and decreasing the rate of the steering inversion (Figure 6C). Silencing L4 and Lawf1 neurons also abolished the inversion of reverse-optomotor responses (Figure 6C). These disparate phenotypes suggest that several different lamina neuron types differentially influence the time course of visual adaptation. We note that related feedback neuron pairs (C2/C3 and Lawf1/Lawf2) appear to exert opposing effects.

Both behavioral responses and the activity of motion-sensitive neurons are known to depend on the temporal frequency of the motion stimulus (Borst et al., 2010). To closely explore temporal tuning of motion circuits, we employed a psychophysical technique known as motion nulling (Chichilnisky et al., 1993; Smeets et al., 2007), in which two motion gratings are superimposed—a reference pattern moving in one direction and a test pattern moving in the opposite direction. We tested the ability of flies to distinguish between high- and low-contrast motion stimuli by varying the velocity and contrast of the test pattern across trials. We quantified contrast sensitivity as a function of stimulus velocity by determining the “null contrast” at each test speed (Figure 7A). The null contrast level of control flies varied as a function of the test pattern velocity, providing a measure of contrast sensitivity across stimulus speeds (black line, Figure 7B). Because the reference pattern remained constant (and at a speed close to *Drosophila*’s temporal frequency optimum), peak contrast sensitivity occurred when the reference and test pattern were moving at the same speed (5.33 Hz).

(D) Same as in (F) but for feedback neurons that contribute significantly to contrast sensitivity tuning. The neuron classes shown here represent all of the individual cell types for which the null contrast of at least two temporal frequencies is significant at the $p < 0.1$ level or lower (details in Supplemental Experimental Procedures).

(E) Summary of the changes in temporal tuning: inactivating L1, L2, and L4 leads to enhanced contrast sensitivity at lower frequencies and reduced sensitivity at higher frequencies, L3 inactivation leads to the opposite phenotype, and the feedback cells only affect the flies’ contrast sensitivity at lower frequencies.

(F) A model for lamina processing with parallel inputs to an HR-EMD, representing the L1, L2/L4, and L3 pathways. L1 and L2/L4 preprocessing were modeled as fast pathways (with identical low-pass filters with time constants of $\tau = 4$ ms), while the L3 input was modeled as a much slower pathway (low-pass filter with $\tau = 80$ ms). The remainder of the model is a standard HR-EMD (with the delay implemented as a low-pass filter with $\tau = 18$ ms; see Supplemental Experimental Procedures for details of the simulation).

(G) Simulated responses of this model to the identical stimuli used in the motion nulling behavioral experiments capture the general changes in temporal tuning seen in (C). Removing either L1 or L2/L4 pathway input resulted in enhanced contrast sensitivity to low-frequency stimuli and a reduction in the high-frequency sensitivity, while removing the L3 input lead to the opposite phenotype.

Silencing four of the five lamina output neuron types (the feed-forward pathway) had a strong effect on the shape of contrast sensitivity tuning curves. For example, silencing L3 neurons increased the tendency of flies to follow high-velocity, low-contrast patterns (Figure 7B), which extended the height of the contrast sensitivity tuning function (Figure 7C). In comparison, silencing L1, L2, and L4 resulted in a compression of the contrast sensitivity tuning functions (Figure 7C).

Silencing three of the four types of feedback neurons, C2, C3, and Lawf2, affected the ability of flies to distinguish small contrast differences at low test speeds, while behavior at higher test speeds remained normal. Interestingly, manipulating lamina output neurons reveals an imbalance (when compared to the control response) between contrast discrimination at high and low speeds (Figures 7C and 7E). In other words, amplified sensitivity in one speed range was accompanied by decreased sensitivity at other speeds. To explore this apparent trade-off and to identify mechanisms that could recapitulate these inactivation results, we simulated lamina processing as the input to a classic HR-EMD (Figure 7C). We observed this imbalanced response with simulations in which the L1 and L2/L4 pathways were tuned differently than the L3 pathway. Specifically, we set the L1 and L2/L4 pathways to be identical and significantly faster than L3 (Figure 7F). When we simulated this model (detailed in Supplemental Experimental Procedures) for the stimulus conditions used in the behavioral experiments of Figure 7C, we found a general agreement between the shape of the temporal tuning curves, as well as the effects of inactivating the faster (L1 or L2/L4) or slower (L3) input pathways.

In contrast to lamina output neurons, manipulation of lamina-associated feedback neurons specifically altered contrast sensitivity at low speeds (Figures 7D and 7E). This distinction is consistent with basic principles from control theory that stable closed-loop systems require low-frequency, bandwidth-limited feedback signals (Csete and Doyle, 2002).

DISCUSSION

In this study, we combined psychophysical measurements with targeted genetic manipulations in order to understand how lamina-associated neurons in *Drosophila* shape visual perception. By testing a wide range of visual behaviors, we identified distinct behavioral phenotypes for 11 out of the 12 neuron types that innervate the lamina (Figures 4A and 4B). Overall, our results suggest that the critical elements of motion detection probably reside downstream of the lamina but that lamina neurons play an important role in shaping the input signals to motion circuits.

We were surprised to find that silencing several lamina neuron classes altered fly responses to asymmetric motion stimuli (i.e., progressive versus regressive). Models for fly motion detection typically assume that visual circuits are organized symmetrically across the eye. However, for four cell types, L2, L4, C2, and C3, we found behavioral phenotypes that depended on the direction of stimulus motion. L4, C2, and C3 are the only columnar lamina-associated neurons that extend across multiple retinotopic columns in the medulla, and L2 provides the primary inputs into L4. These extensions are consistently asymmetric with respect

to the coordinates of the eye, suggesting a mechanistic correlation between anatomy and function. For example, we found that C3 arbors in layer M9 of the medulla innervate more posterior columns, consistent with our finding that silencing C3 neurons produced striking deficits in the perception of regressive motion. One possibility is that feedback from more posterior columns onto more anterior columns would augment the response of the more anterior column to an edge moving regressively. Responses to edge stimuli moving in the opposite direction progressively would not be affected. C2 and C3 also make connections in the medulla, where they could affect processing in downstream circuits. Distinguishing between these hypotheses will require physiological recordings from C2 and C3 neurons, or recordings from LMC neurons while manipulating centrifugal neuron feedback. Similarly, recording from L2 neurons while silencing L4 neurons will provide insight into how L4 contributes to progressive motion processing.

Our data suggest that several features previously attributed to visual motion computation may result from processing in peripheral premotion circuits. For example, an important prediction of the HR-EMD model is that the time constant of the delay line shapes the temporal tuning of fly motion detection and thus the shape of the optomotor response curve (Figures 1B and 3C; Reichardt, 1961). However, we found that silencing some lamina neurons (L1, L2, and L4) specifically decreased the tendency of flies to follow very fast motion stimuli, while silencing L3 had the opposite effect, increasing fly responses to fast motion stimuli (Figure 7C). Consistent with our behavioral and simulation results, L3 neurons in larger flies have a higher input resistance than L1 or L2 (Hardie and Weckström, 1990), which could result in attenuation of high-frequency signals in L3 (although this attenuation may also occur in neurons downstream of L3).

The simulation results of Figures 7F and 7G strongly suggest that processing by individual cell types (and subsequent downstream pathways) contribute to the aggregate tuning of motion vision. Specifically, the temporal frequency optimum of the elaborated HR-EMD (Figure 7F) is no longer determined strictly by the time constant of the delay line but is affected by the time constants of the input pathways as well (and would be further influenced by the dynamics of feedback pathways if included in the model). This simulation illustrates one example of a potentially general principle of the fly lamina: anatomically related cell types carry out similar functions but with distinct temporal properties. The two classes of reverse-optomotor phenotypes (Figure 6) suggest that L2 and L4, C2 and C3, and Lawf1 and Lawf2 may in each case represent two “arms” of a balanced network. The duplication of function with temporal specializations that we propose need not be independent (as in our model of Figure 7F) from the recently described bifurcation into pathways specialized for the detection of luminance increments and decrements (Joesch et al., 2013). Overall the diverse range of phenotypes related to motion responses at different speeds (Figures 6 and 7) suggests that many lamina cell types contribute to shaping the temporal tuning of early visual processing. By structuring the inputs to downstream motion circuits, lamina neurons appear to play an important role in shaping the tuning of visual behaviors, such as the optomotor response, that have previously been

compactly described by the HR-EMD model. These observations provide one possible explanation for the apparent mismatch between the minimal complexity of motion detection models and the elaborate diversity of lamina and medulla neuron classes.

Our data also do not support the hypothesis that specific lamina neurons serve as dedicated pathways for encoding global stimulus features, such as patterns of optic flow. Rather, a small number of neuron types, mainly L1 and L2, are essential for basic motion detection, while the majority of lamina neuron types serve to dynamically sculpt and enhance these feedforward signals. For example, we discovered that four classes of feedback neurons, the centrifugal neurons C2 and C3 and the wide-field neurons Lawf1 and Lawf2, play an intimate role in visual motion processing. These feedback projections from the medulla could mediate adaptation, gain control, or behavioral state modulation of the lamina neurons that provide input to motion circuits.

Our results suggest that lateral interactions between retinotopic columns and feedback from downstream neurons both play an important role in shaping visual motion detection. These pathways may serve to enhance the coding capacity of motion pathways through adaptation mechanisms previously identified in the lamina, such as predictive gain control (Srinivasan et al., 1982) and lateral inhibition (Laughlin et al., 1987). For example, the reduced sensitivity to low-contrast and fast-motion stimuli we observed in L4 silencing experiments (Figures 4A and S7A) could result from decreased lateral interactions within the lamina and a consequent decrease in coding efficiency. Similarly, feedback from the centrifugal neurons C2 and C3 could enhance detection of unexpected regressive motion signals (Zabala et al., 2012) by integrating signals from neighboring posterior columns in the medulla.

We found that specific spatial and temporal features of fly motion perception can be separated using targeted genetic manipulations of lamina neurons. This suggests that the HR-EMD model may be implemented in a more distributed manner than previously thought, possibly involving parallel circuits that rely on contributions from many neuronal cell types in the lamina and medulla. Several recent studies have reached similar conclusions, for example, proposing that parallel motion circuits exist for detecting ON- and OFF-type edges (Clark et al., 2011; Joesch et al., 2010, 2013). Although we did not find evidence for lamina neurons providing strong rectification into ON and OFF input channels, this is most likely due to differences in behavioral assays and not differences in GAL4 lines or neural effectors (Figure S6). It is also possible that some visual stimuli used in this study activated multiple, parallel motion circuits, which could mask the effects of silencing a single neuron class. This could be tested in the future by silencing other specific combinations of closely related lamina neurons, such as L2 and L4 or L1 and L3.

Previous studies of the lamina have used different neural effectors, in particular a temperature-sensitive dynamin mutant (Shibire^{ts}) (Kitamoto, 2001), to silence neurons (Clark et al., 2011; Joesch et al., 2010; Rister et al., 2007). We chose to use the Kir2.1 channel because its expression permitted sustained flight behavior for long periods (enabling the comparative study of many visual stimuli), which is not possible at the higher tem-

peratures required for Shibire^{ts}. Because the Kir2.1 channel is tagged with GFP, we were also able to verify its expression and efficacy (Figure S3). One caveat of this approach is that Kir2.1 expression hyperpolarizes the resting potential, which could affect neighboring neurons through electrical gap junctions. Because gap junctions in the fly nervous system are not detectable by electron microscopy, their frequency and distribution in the visual system are not well understood (Meinertzhagen and O'Neil, 1991; Rivera-Alba et al., 2011). However, there is some evidence for their existence in the lamina, for example between L1 and L2 (Joesch et al., 2010). Two pieces of evidence indicate that the Kir2.1 expression in our experiments did not affect multiple cell types. First, we observed unique and specific phenotypes for most of the cell types examined. Second, for those cases in which we silenced neuron pairs (L1/L2 and C2/C3), we observed stronger phenotypes when we manipulated both cells compared to the component neurons. Nonetheless, it is still possible that Kir2.1 expression enhances the deficits we report by affecting electrically coupled neurons, and future experiments using improved neural effectors will be required to test this possibility.

A common approach to probe the functional role of neuronal cell types is to selectively silence or activate small subsets of neurons and then examine the resultant effects on behavior. Though this approach is widely used in *Drosophila* and other genetic model organisms, its utility has been limited by two main experimental challenges. First, highly specific genetic driver lines have been unavailable for most cell populations. This has made it difficult to confidently attribute observed behavioral phenotypes to the manipulation of individual cell types. Second, the behavioral assays applied have often been too limited to reveal potential functions for most of the neuronal classes examined. Our results for the fly lamina show that it is possible to use intersectional genetic techniques to systematically target all the neuronal cell types in a brain region of interest. Furthermore, we show that diverse quantitative behavioral assays can reveal functional roles for nearly all examined neuronal classes. With the recent availability of a large collection of defined GAL4 driver lines (Jenett et al., 2012), this approach can now be readily applied to other parts of the *Drosophila* brain.

EXPERIMENTAL PROCEDURES

Split-GAL4 transgenes were selected based on GAL4-line expression patterns (Jenett et al., 2012), constructed as previously described in Pfeiffer et al. (2010) and listed in Table S1. Expression patterns of Split-GAL4 lines were assessed by anti-GFP antibody staining and confocal imaging of 5- to 10-day-old female flies expressing one of two different UAS reporters. A “flip-out”-based approach (Struhl and Basler, 1993) was used for stochastic single-cell labeling.

For all tethered flight experiments, we used female *Drosophila* (3–5 days old), which were heterozygous for both GAL4 and UAS transgenes (effectors backcrossed into Dickinson Laboratory [DL] or Canton-S [CS] wild-type backgrounds). Each fly was tethered to a tungsten wire with UV-cured glue and suspended within an electronic visual flight simulator consisting of a 32 × 88 cylindrical array of green LEDs (Reiser and Dickinson, 2008). The amplitude and frequency of the fly's wing beats were monitored with an optical wing-beat analyzer, allowing us to present visual stimuli in either open- or closed-loop mode (Götz, 1987). All visual stimuli are described in the Supplemental Experimental Procedures and depicted in Figure S2. Each 3 s open-loop

stimulus condition was followed by 3.5 s of closed-loop “stripe fixation” to ensure that flies were actively steering at the onset of each trial. Within an experiment, each set of conditions was presented as random blocks repeated three times. Trials in which the fly stopped flying were repeated at the end of each block. These data were averaged on a per fly basis to produce a mean turning response for each stimulus condition. Further details of the all methods used are provided in the [Supplemental Experimental Procedures](#).

SUPPLEMENTAL INFORMATION

Supplemental Information includes seven figures, one table, and Supplemental Experimental Procedures and can be found with this article online at <http://dx.doi.org/10.1016/j.neuron.2013.05.024>.

ACKNOWLEDGMENTS

We thank Barret Pfeiffer, Heather Dionne, and Chris Murphy for molecular biology of Split-GAL4 constructs, Teri Ngo and Ming Wu for assistance with Split-GAL4 screening, the Janelia Fly Core for assistance with *Drosophila* care, the Janelia Fly Light Project for providing images of the primary GAL4 lines and of C2 single neurons, the Janelia Fly Light Scientific Computing Team for image processing software, Matt Smear and Stephen Huston for assistance with stimulus design, Damon Clark for discussions of L1- and L2-inactivation phenotypes, and Magnus Karlsson and Jinyang Liu for continued development and support of the visual display system. The Iso-D1 and the two L1 stocks used in Figure S6 were a gift from Tom Clandinin. We also thank Larry Zipursky, Alla Karpova, Stefan Pulver, Vivek Jayaraman, Anthony Leonardo, and members of the Reiser, Jayaraman, Card, and Rubin laboratories. This project was supported by HHMI.

Accepted: May 10, 2013

Published: June 20, 2013

REFERENCES

- Anstis, S.M., and Rogers, B.J. (1975). Illusory reversal of visual depth and movement during changes of contrast. *Vision Res.* *15*, 957–961.
- Baines, R.A., Uhler, J.P., Thompson, A., Sweeney, S.T., and Bate, M. (2001). Altered electrical properties in *Drosophila* neurons developing without synaptic transmission. *J. Neurosci.* *21*, 1523–1531.
- Benjamini, Y., and Hochberg, Y. (1995). Controlling the false discovery rate: a practical and powerful approach to multiple testing. *J. R. Stat. Soc. Ser. B-Methodol.* *57*, 289–300.
- Borst, A., and Euler, T. (2011). Seeing things in motion: models, circuits, and mechanisms. *Neuron* *71*, 974–994.
- Borst, A., Haag, J., and Reiff, D.F. (2010). Fly motion vision. *Annu. Rev. Neurosci.* *33*, 49–70.
- Braitenberg, V. (1967). Patterns of projection in the visual system of the fly. I. Retina-lamina projections. *Exp. Brain Res.* *3*, 271–298.
- Braitenberg, V., and Debbage, P. (1974). A regular net of reciprocal synapses in the visual system of the fly, *Musca domestica*. *J. Comp. Physiol. A Neuroethol. Sens. Neural Behav. Physiol.* *90*, 25–31.
- Buchner, E. (1971). *Dunkelanregung des stationären Flugs der Fruchtfliege Drosophila*. PhD thesis, University of Tübingen, Tübingen, Germany.
- Buchner, E. (1976). Elementary movement detectors in an insect visual system. *Biol. Cybern.* *24*, 85–101.
- Buchner, E. (1984). Behavioural analysis of spatial vision in insects. In *Photoreception and Vision in Invertebrates*, M. Ali, ed. (New York: Plenum), pp. 561–619.
- Carver, S., Roth, E., Cowan, N.J., and Fortune, E.S. (2008). Synaptic plasticity can produce and enhance direction selectivity. *PLoS Comput. Biol.* *4*, e32.
- Cavanagh, P., and Anstis, S. (1991). The contribution of color to motion in normal and color-deficient observers. *Vision Res.* *31*, 2109–2148.
- Chichilnisky, E.J., Heeger, D., and Wandell, B.A. (1993). Functional segregation of color and motion perception examined in motion nulling. *Vision Res.* *33*, 2113–2125.
- Clark, D.A., Bursztyn, L., Horowitz, M.A., Schnitzer, M.J., and Clandinin, T.R. (2011). Defining the computational structure of the motion detector in *Drosophila*. *Neuron* *70*, 1165–1177.
- Coombe, P.E., Srinivasan, M.V., and Guy, R.G. (1989). Are the large monopolar cells of the insect lamina on the optomotor pathway? *J. Comp. Physiol. A Neuroethol. Sens. Neural Behav. Physiol.* *166*, 23–35.
- Csete, M.E., and Doyle, J.C. (2002). Reverse engineering of biological complexity. *Science* *295*, 1664–1669.
- Douglass, J.K., and Strausfeld, N.J. (1995). Visual motion detection circuits in flies: peripheral motion computation by identified small-field retinotopic neurons. *J. Neurosci.* *15*, 5596–5611.
- Duistermars, B.J., Chow, D.M., Condro, M., and Frye, M.A. (2007a). The spatial, temporal and contrast properties of expansion and rotation flight optomotor responses in *Drosophila*. *J. Exp. Biol.* *210*, 3218–3227.
- Duistermars, B.J., Reiser, M.B., Zhu, Y., and Frye, M.A. (2007b). Dynamic properties of large-field and small-field optomotor flight responses in *Drosophila*. *J. Comp. Physiol. A Neuroethol. Sens. Neural Behav. Physiol.* *193*, 787–799.
- Duistermars, B.J., Care, R.A., and Frye, M.A. (2012). Binocular interactions underlying the classic optomotor responses of flying flies. *Front. Behav. Neurosci.* *6*, 6.
- Egelhaaf, M., and Borst, A. (1989). Transient and steady-state response properties of movement detectors. *J. Opt. Soc. Am. A* *6*, 116–127.
- Eichner, H., Joesch, M., Schnell, B., Reiff, D.F., and Borst, A. (2011). Internal structure of the fly elementary motion detector. *Neuron* *70*, 1155–1164.
- Farrow, K., Haag, J., and Borst, A. (2006). Nonlinear, binocular interactions underlying flow field selectivity of a motion-sensitive neuron. *Nat. Neurosci.* *9*, 1312–1320.
- Fei, H., Chow, D.M., Chen, A., Romero-Calderón, R., Ong, W.S., Ackerson, L.C., Maidment, N.T., Simpson, J.H., Frye, M.A., and Krantz, D.E. (2010). Mutation of the *Drosophila* vesicular GABA transporter disrupts visual figure detection. *J. Exp. Biol.* *213*, 1717–1730.
- Fischbach, K.F., and Dittrich, A.P. (1989). The optic lobe of *Drosophila melanogaster*. I. A Golgi analysis of wild-type structure. *Cell Tissue Res.* *258*, 441–475.
- Gao, S., Takemura, S.Y., Ting, C.Y., Huang, S., Lu, Z., Luan, H., Rister, J., Thum, A.S., Yang, M., Hong, S.T., et al. (2008). The neural substrate of spectral preference in *Drosophila*. *Neuron* *60*, 328–342.
- Gollisch, T., and Meister, M. (2010). Eye smarter than scientists believed: neural computations in circuits of the retina. *Neuron* *65*, 150–164.
- Götz, K.G. (1964). Optomotorische Untersuchung des visuellen Systems einiger Augenmutanten der Fruchtfliege *Drosophila*. *Kybernetik* *2*, 77–92.
- Götz, K.G. (1968). Flight control in *Drosophila* by visual perception of motion. *Kybernetik* *4*, 199–208.
- Götz, K.G. (1987). Course-control, metabolism and wing interference during ultralong tethered flight in *Drosophila melanogaster*. *J. Exp. Biol.* *128*, 35–46.
- Haag, J., Denk, W., and Borst, A. (2004). Fly motion vision is based on Reichardt detectors regardless of the signal-to-noise ratio. *Proc. Natl. Acad. Sci. USA* *101*, 16333–16338.
- Hamada, F.N., Rosenzweig, M., Kang, K., Pulver, S.R., Ghezzi, A., Jegla, T.J., and Garrity, P.A. (2008). An internal thermal sensor controlling temperature preference in *Drosophila*. *Nature* *454*, 217–220.
- Hardie, R.C., and Weckström, M. (1990). Three classes of potassium channels in large monopolar cells of the blowfly *Calliphora vicina*. *J. Comp. Physiol. A Neuroethol. Sens. Neural Behav. Physiol.* *167*, 723–736.
- Hasegawa, E., Kitada, Y., Kaido, M., Takayama, R., Awasaki, T., Tabata, T., and Sato, M. (2011). Concentric zones, cell migration and neuronal circuits in the *Drosophila* visual center. *Development* *138*, 983–993.

- Hassenstein, V.B., and Reichardt, W. (1956). Systemtheoretische Analyse der Zeit-, Reihenfolgen und Vorzeichenbewertung bei der Bewegungsperzeption des Rüsselkäfers *Chlorophanus*. *Z Naturforsch* 11b, 513–524.
- Hausen, K. (1982). Motion sensitive interneurons in the optomotor system of the fly. II. The horizontal cells: receptive-field organization and response characteristics. *Biol. Cybern.* 46, 67–79.
- Hausen, K., and Wehrhahn, C. (1989). Neural circuits mediating visual flight control in flies. I. Quantitative comparison of neural and behavioral response characteristics. *J. Neurosci.* 9, 3828–3836.
- Heisenberg, M. (1972). Comparative behavioral studies on 2 visual mutants of *Drosophila*. *J. Comp. Physiol. A Neuroethol. Sens. Neural Behav. Physiol.* 80, 119–136.
- Heisenberg, M., and Wolf, R. (1984). *Vision in Drosophila: Genetics of Microbehavior* (Berlin: Springer-Verlag).
- Helfrich-Förster, C., Shafer, O.T., Wülbeck, C., Grieshaber, E., Rieger, D., and Taghert, P. (2007). Development and morphology of the clock-gene-expressing lateral neurons of *Drosophila melanogaster*. *J. Comp. Neurol.* 500, 47–70.
- Jenett, A., Rubin, G.M., Ngo, T.T., Shepherd, D., Murphy, C., Dionne, H., Pfeiffer, B.D., Cavallaro, A., Hall, D., Jeter, J., et al. (2012). A GAL4-driver line resource for *Drosophila* neurobiology. *Cell Rep* 2, 991–1001.
- Joesch, M., Schnell, B., Raghu, S.V., Reiff, D.F., and Borst, A. (2010). ON and OFF pathways in *Drosophila* motion vision. *Nature* 468, 300–304.
- Joesch, M., Weber, F., Eichner, H., and Borst, A. (2013). Functional specialization of parallel motion detection circuits in the fly. *J. Neurosci.* 33, 902–905.
- Katsov, A.Y., and Clandinin, T.R. (2008). Motion processing streams in *Drosophila* are behaviorally specialized. *Neuron* 59, 322–335.
- Kirschfeld, K. (1967). Die Projektion der optischen Umwelt auf das Raster der Rhabdomere im Komplexauge von *MUSCA*. *Exp. Brain Res.* 3, 248–270.
- Kitamoto, T. (2001). Conditional modification of behavior in *Drosophila* by targeted expression of a temperature-sensitive shibire allele in defined neurons. *J. Neurobiol.* 47, 81–92.
- Kolodziejczyk, A., Sun, X., Meinertzhagen, I.A., and Nässel, D.R. (2008). Glutamate, GABA and acetylcholine signaling components in the lamina of the *Drosophila* visual system. *PLoS ONE* 3, e2110.
- Krapp, H.G., Hengstenberg, B., and Hengstenberg, R. (1998). Dendritic structure and receptive-field organization of optic flow processing interneurons in the fly. *J. Neurophysiol.* 79, 1902–1917.
- Krapp, H.G., Hengstenberg, R., and Egelhaaf, M. (2001). Binocular contributions to optic flow processing in the fly visual system. *J. Neurophysiol.* 85, 724–734.
- Laughlin, S.B., and Hardie, R.C. (1978). Common strategies for light adaptation in the peripheral visual systems of fly and dragonfly. *J. Comp. Physiol. A Neuroethol. Sens. Neural Behav. Physiol.* 128, 319–340.
- Laughlin, S.B., Howard, J., and Blakeslee, B. (1987). Synaptic limitations to contrast coding in the retina of the blowfly *Calliphora*. *Proc. R. Soc. Lond. B Biol. Sci.* 237, 437–467.
- Luan, H., Peabody, N.C., Vinson, C.R., and White, B.H. (2006). Refined spatial manipulation of neuronal function by combinatorial restriction of transgene expression. *Neuron* 52, 425–436.
- Meinertzhagen, I.A., and O'Neil, S.D. (1991). Synaptic organization of columnar elements in the lamina of the wild type in *Drosophila melanogaster*. *J. Comp. Neurol.* 305, 232–263.
- Pfeiffer, B.D., Jenett, A., Hammonds, A.S., Ngo, T.T., Misra, S., Murphy, C., Scully, A., Carlson, J.W., Wan, K.H., Laverty, T.R., et al. (2008). Tools for neuroanatomy and neurogenetics in *Drosophila*. *Proc. Natl. Acad. Sci. USA* 105, 9715–9720.
- Pfeiffer, B.D., Ngo, T.T., Hibbard, K.L., Murphy, C., Jenett, A., Truman, J.W., and Rubin, G.M. (2010). Refinement of tools for targeted gene expression in *Drosophila*. *Genetics* 186, 735–755.
- Pulver, S.R., Pashkovski, S.L., Hornstein, N.J., Garrity, P.A., and Griffith, L.C. (2009). Temporal dynamics of neuronal activation by Channelrhodopsin-2 and TRPA1 determine behavioral output in *Drosophila* larvae. *J. Neurophysiol.* 101, 3075–3088.
- Reichardt, W. (1961). Autocorrelation, a principle for the evaluation of sensory information by the central nervous system. In *Sensory Communication*, W.A. Rosenblith, ed. (New York: John Wiley), pp. 303–317.
- Reichardt, W., and Wenking, H. (1969). Optical detection and fixation of objects by fixed flying flies. *Naturwissenschaften* 56, 424–425.
- Reiff, D.F., Plett, J., Mank, M., Griesbeck, O., and Borst, A. (2010). Visualizing retinotopic half-wave rectified input to the motion detection circuitry of *Drosophila*. *Nat. Neurosci.* 13, 973–978.
- Reiser, M.B., and Dickinson, M.H. (2008). A modular display system for insect behavioral neuroscience. *J. Neurosci. Methods* 167, 127–139.
- Rister, J., Pauls, D., Schnell, B., Ting, C.Y., Lee, C.H., Snakevitch, I., Morante, J., Strausfeld, N.J., Ito, K., and Heisenberg, M. (2007). Dissection of the peripheral motion channel in the visual system of *Drosophila melanogaster*. *Neuron* 56, 155–170.
- Rivera-Alba, M., Vitaladevuni, S.N., Mishchenko, Y., Lu, Z., Takemura, S.Y., Scheffer, L., Meinertzhagen, I.A., Chklovskii, D.B., and de Polavieja, G.G. (2011). Wiring economy and volume exclusion determine neuronal placement in the *Drosophila* brain. *Curr. Biol.* 21, 2000–2005.
- Single, S., and Borst, A. (1998). Dendritic integration and its role in computing image velocity. *Science* 281, 1848–1850.
- Single, S., Haag, J., and Borst, A. (1997). Dendritic computation of direction selectivity and gain control in visual interneurons. *J. Neurosci.* 17, 6023–6030.
- Smear, M.C., Tao, H.W., Staub, W., Orger, M.B., Gosse, N.J., Liu, Y., Takahashi, K., Poo, M.M., and Baier, H. (2007). Vesicular glutamate transport at a central synapse limits the acuity of visual perception in zebrafish. *Neuron* 53, 65–77.
- Srinivasan, M.V., Laughlin, S.B., and Dubs, A. (1982). Predictive coding: a fresh view of inhibition in the retina. *Proc. R. Soc. Lond. B Biol. Sci.* 216, 427–459.
- Strausfeld, N.J., and Campos-Ortega, J.A. (1973). The L4 monopolar neurone: a substrate for lateral interaction in the visual system of the fly *Musca domestica* (L.). *Brain Res.* 59, 97–117.
- Struhl, G., and Basler, K. (1993). Organizing activity of wingless protein in *Drosophila*. *Cell* 72, 527–540.
- Takemura, S.Y., Lu, Z., and Meinertzhagen, I.A. (2008). Synaptic circuits of the *Drosophila* optic lobe: the input terminals to the medulla. *J. Comp. Neurol.* 509, 493–513.
- Takemura, S.Y., Karuppururai, T., Ting, C.Y., Lu, Z., Lee, C.H., and Meinertzhagen, I.A. (2011). Cholinergic circuits integrate neighboring visual signals in a *Drosophila* motion detection pathway. *Curr. Biol.* 21, 2077–2084.
- Tammero, L.F., Frye, M.A., and Dickinson, M.H. (2004). Spatial organization of visuomotor reflexes in *Drosophila*. *J. Exp. Biol.* 207, 113–122.
- Theobald, J.C., Ringach, D.L., and Frye, M.A. (2010). Dynamics of optomotor responses in *Drosophila* to perturbations in optic flow. *J. Exp. Biol.* 213, 1366–1375.
- Tuthill, J.C., Chiappe, M.E., and Reiser, M.B. (2011). Neural correlates of illusory motion perception in *Drosophila*. *Proc. Natl. Acad. Sci. USA* 108, 9685–9690.
- Zabala, F., Polidoro, P., Robie, A., Branson, K., Perona, P., and Dickinson, M.H. (2012). A simple strategy for detecting moving objects during locomotion revealed by animal-robot interactions. *Curr. Biol.* 22, 1344–1350.
- Zheng, L., de Polavieja, G.G., Wolfram, V., Asyali, M.H., Hardie, R.C., and Juusola, M. (2006). Feedback network controls photoreceptor output at the layer of first visual synapses in *Drosophila*. *J. Gen. Physiol.* 127, 495–510.
- Zhu, Y., Nern, A., Zipursky, S.L., and Frye, M.A. (2009). Peripheral visual circuits functionally segregate motion and phototaxis behaviors in the fly. *Curr. Biol.* 19, 613–619.